Monochromatic Scattering from Three-Dimensional Gyrotropic Bodies Using the TLM Method

Ahmet F. Yagli[1], Jay K. Lee[2], and Ercument Arvas[2]

(1) Turksat A.S.
Konya Yolu 40.km Golbasi, Ankara, Turkey
afyagli@turksat.com.tr
(2) Department of Electrical Engineering and Computer Science
Syracuse University, Syracuse, NY 13244, USA
leejk@syr.edu, earvas@syr.edu

Abstract – A three-dimensional scattering field Transmission Line Modeling (TLM) algorithm is established to obtain bistatic radar cross sections of gyroelectric and gyromagnetic objects at a single frequency. Although gyrotropic material properties are highly frequency dependent, their permittivity and permeability tensors are made of complex constants at a given frequency. For verification, the results for gyrotropic spheres are compared with those from previous studies, in which an analytical approach and the Method of Moments along with Conjugant Gradient Fast Fourier Transform method were used.

Index terms – Gyrotropic material, Scattering, Transmission Line Modeling (TLM).

I. INTRODUCTION

Obtaining the electromagnetic scattering of three dimensional homogeneous gyrotropic objects is the main goal of this paper. Previously, there have been some studies regarding the radar cross sections of two dimensional or three dimensional anisotropic materials. An analytical solution of electromagnetic fields in homogeneous plasma anisotropic media is given by Geng et al. [1]. They displayed some numerical results of scattering from gyroelectric spheres. Geng and Wu [2] showed an analytical solution of the scattering fields of a ferrite sphere by a plane wave using spherical vector-wave function. They compare some of their numerical results for radar cross sections of gyromagnetic spheres with MoM CG-FFT simulation results of Zhu et al. [3].

Differential time domain methods such as the finite difference time domain (FDTD) method [4] or the transmission line modeling (TLM) method [5] are widely used for modeling electromagnetic problems consisting of complex materials with arbitrarily shaped structures. The main difference between the two techniques is the layout of the unit cell and the time-stepping process [6,7]. In this paper, we derive a scattering field 3D TLM formulation from Paul's algorithm discussed in Reference [6]. Paul's TLM algorithm is a total field formulation, in which it was difficult to generate a perfect plane wave as our incident wave. We needed to obtain the scattering field formulation, where the incident wave is analytically injected to the computation space. Since our TLM computation space is truncated, a near field to far field transformation method is also used to obtain the far field scattering [8,9].

We describe the TLM algorithm used for modeling 3D gyrotropic objects in this study. Then the simulation results of gyrotropic spheres, cubes, and finite cylinders are demonstrated. Our TLM simulation results for gyrotropic spheres are validated by the currently available alternative methods.

II. GYROTROPIC MEDIA

Gyrotropic media have been an important research topic because of their anisotropic and nonreciprocal behavior. When subjected to a constant magnetic field, both plasmas and ferrites, which exist in nature, exhibit anisotropic constitutive parameters. Plasmas and ferrites under the influence of the applied magnetic field, are generally called magnetized plasmas (or magnetoplasmas) and magnetized ferrites respectively. For magnetized plasmas the anisotropy is described by using a permittivity tensor instead of a scalar permittivity, because of their rich free electron content. On the other hand, magnetized ferrites are characterized by a permeability tensor in place of a scalar permeability value. In ferrites, the anisotropic behavior is due to the magnetic dipole moments, which form the structure of the material.

A good example for magnetized plasmas is the earth's ionosphere layer, where the free electrons and charged ions are greatly affected by the earth's magnetic field between the two poles. We can see the ionosphere as a free electron gas around a huge magnet. There is a wide variety of usage for ferrite devices, from telecommunication to military applications.

A gyrotropic medium is called *electrically gyrotropic* or *gyroelectric* if the medium is characterized by a relative permittivity tensor and a constant permeability value. If we write the constant magnetic field as $\overline{B}_0 = \hat{b}_0 B_0$, where the unit vector $\hat{b}_0$ shows the direction of the field vector, the relative permittivity and permeability tensors of a gyroelectric medium can be expressed in the following dyadic form

$$\overline{\overline{\varepsilon}} = \varepsilon_1 \left(\overline{\overline{I}} - \hat{b}_0\hat{b}_0\right) - j\varepsilon_2 \left(\hat{b}_0 \times \overline{\overline{I}}\right) + \varepsilon_3 \hat{b}_0\hat{b}_0 \ , \ \overline{\overline{\mu}} = \mu\overline{\overline{I}}. \tag{1}$$

In this equation $\overline{\overline{I}}$ is the unit matrix, which has value of 1 at diagonal elements and 0 at off-diagonal elements, and j is $\sqrt{-1}$. In this study the time variation of field components is taken as $e^{j\omega t}$.

When a medium is characterized by a relative permeability tensor and a constant permittivity value, the medium is called *magnetically gyrotropic* or *gyromagnetic*. The relative permittivity and permeability tensors of a gyromagnetic medium can be expressed in the following dyadic form

$$\overline{\overline{\mu}} = \mu_1 \left(\overline{\overline{I}} - \hat{b}_0\hat{b}_0\right) - j\mu_2 \left(\hat{b}_0 \times \overline{\overline{I}}\right) + \mu_3 \hat{b}_0\hat{b}_0 \ , \ \overline{\overline{\varepsilon}} = \varepsilon\overline{\overline{I}}. \tag{2}$$

Reference [10] discusses dyadic tensor and vector operations in detail.

In the Cartesian coordinate system, if $\overline{B}_0 = \hat{z}B_0$, the relative permittivity and permeability tensors can be obtained as

$$\overline{\overline{\varepsilon}} = \begin{bmatrix} \varepsilon_1 & j\varepsilon_2 & 0 \\ -j\varepsilon_2 & \varepsilon_1 & 0 \\ 0 & 0 & \varepsilon_3 \end{bmatrix} \tag{3}$$

and

$$\overline{\overline{\mu}} = \begin{bmatrix} \mu_1 & j\mu_2 & 0 \\ -j\mu_2 & \mu_1 & 0 \\ 0 & 0 & \mu_3 \end{bmatrix}. \tag{4}$$

For example, if the medium is a magnetoplasma, which is a gyroelectric medium, then the permittivity tensor parameters are given by [11]

$$\varepsilon_1 = 1 - \frac{\omega_p^2(\omega - j\nu_c)}{\omega\left[(\omega - j\nu_c)^2 - \omega_b^2\right]}, \tag{5a}$$

$$\varepsilon_2 = -\frac{\omega_p^2\omega_b}{\omega\left[(\omega - j\nu_c)^2 - \omega_b^2\right]}, \tag{5b}$$

$$\varepsilon_3 = 1 - \frac{\omega_p^2}{\omega^2 - j\omega\nu_c} \tag{5c}$$

where ω_b is the gyrofrequency or cyclotron frequency, ω_p is the plasma frequency, and ν_c is the electron collision frequency representing the loss mechanism. (ω is the angular frequency and equal to $2\pi f$.) The cyclotron frequency represents the effect of the applied magnetic field, and is proportional to this static magnetic field

$$\omega_b = -\frac{eB_0}{m}. \tag{6}$$

Here m denotes the mass of each electron with charge e, which is a negative number. The positive number $-e/m$ is called the gyromagnetic ratio.

The plasma frequency can be formulated as

$$\omega_p = \sqrt{\frac{N_0 e^2}{m\varepsilon_0}} \tag{7}$$

where N_0 is the number of free electrons per unit volume.

The effect of collisions, which leads to the absorption of energy, is taken into account by adding the collision frequency into the formulation. These collisions are mainly due to thermal motions. For *cold* plasma, thermal motions are generally neglected, since the distance traversed by an electron is shorter. With $\nu_c = 0$, the parameters of the permittivity tensor of the cold plasma can be written as follows

$$\varepsilon_1 = 1 - \frac{\omega_p^2}{\omega^2 - \omega_b^2}, \tag{8a}$$

$$\varepsilon_2 = -\frac{\omega_p^2\omega_b}{\omega(\omega^2 - \omega_b^2)}, \tag{8b}$$

$$\varepsilon_3 = 1 - \frac{\omega_p^2}{\omega^2}. \tag{8c}$$

The derivations of these parameters are given in [12].

On the other hand if the medium is a magnetized ferrite which is a gyromagnetic medium, then the permeability parameters are defined as [10]

$$\mu_1 = 1 + \frac{\omega_0\omega_m}{\omega_0^2 - \omega^2}, \tag{9a}$$

$$\mu_2 = \frac{\omega\omega_m}{\omega_0^2 - \omega^2}, \tag{9b}$$

$$\mu_3 = 1 \tag{9c}$$

where ω_m is the saturation magnetization frequency, and ω_0 is the Larmor precessional frequency.

III. Scattering Field 3D TLM Modeling of Gyrotropic Media

In his Ph.D dissertation [6] and his paper [7], Paul established a new TLM formulation starting from Maxwell's equations. In his method, the governing field update equation in Laplace domain is

$$2\overline{F}^{e} = 4\overline{F} + \overline{\overline{\sigma}}\,\overline{F} + s\Delta t\, 2\overline{\overline{M}}\,\overline{F} \tag{10}$$

where $\overline{\overline{\sigma}}$ and $\overline{\overline{M}}$ are the conductivity and the susceptibility matrices, respectively ($s = j2\pi f$). $\overline{F}^{e}$ (in Paul's dissertation it is represented as $\overline{F}^{r}$ and called the vector of reflected fields) is the node excitation vector and $\overline{F}$ is the vector of total normalized fields. s is the Laplace variable and Δt stands for the time step duration. Starting from the total field TLM formulation's governing field update equation (10), we can derive the scattering field TLM formulation, which has a field update equation in the form of

$$\begin{aligned} 2\overline{F}^{e}_{scat} &= 4\overline{F}_{scat} + \overline{\overline{\sigma}}\,\overline{F}_{scat} + s\Delta t\, 2\overline{\overline{M}}\,\overline{F}_{scat} \\ &\quad + \overline{\overline{\sigma}}\,\overline{F}_{inc} + s\Delta t\, 2\overline{\overline{M}}\,\overline{F}_{inc} \end{aligned} \tag{11}$$

where $\overline{F}_{scat}$ and $\overline{F}_{inc}$ are the normalized scattered and incident field vectors [13,14].

In our computations, the conductivity matrix $\overline{\overline{\sigma}}$ will be taken as zero. The susceptibility matrix $\overline{\overline{M}}$ has both real and imaginary elements.

Since we assume an applied static magnetic field in z direction, the relative permittivity tensor of the gyroelectric materials has the following form

$$\overline{\overline{\varepsilon}} = \begin{bmatrix} \varepsilon_1 & j\varepsilon_2 & 0 \\ -j\varepsilon_2 & \varepsilon_1 & 0 \\ 0 & 0 & \varepsilon_3 \end{bmatrix} \tag{12}$$

which means an electric susceptibility matrix of

$$\begin{aligned} \overline{\overline{\chi}}_e &= \begin{bmatrix} \chi_{e1} & \chi_{e2} & 0 \\ -\chi_{e2} & \chi_{e1} & 0 \\ 0 & 0 & \chi_{e3} \end{bmatrix} \\ &= \begin{bmatrix} \varepsilon_1 - 1 & j\varepsilon_2 & 0 \\ -j\varepsilon_2 & \varepsilon_1 - 1 & 0 \\ 0 & 0 & \varepsilon_3 - 1 \end{bmatrix}. \end{aligned} \tag{13}$$

Similarly, for gyromagnetic materials, the relative permeability tensor will be given by

$$\overline{\overline{\mu}} = \begin{bmatrix} \mu_1 & j\mu_2 & 0 \\ -j\mu_2 & \mu_1 & 0 \\ 0 & 0 & \mu_3 \end{bmatrix} \tag{14}$$

which implies a magnetic susceptibility matrix of

$$\begin{aligned} \overline{\overline{\chi}}_m &= \begin{bmatrix} \chi_{m1} & \chi_{m2} & 0 \\ -\chi_{m2} & \chi_{m1} & 0 \\ 0 & 0 & \chi_{m3} \end{bmatrix} \\ &= \begin{bmatrix} \mu_1 - 1 & j\mu_2 & 0 \\ -j\mu_2 & \mu_1 - 1 & 0 \\ 0 & 0 & \mu_3 - 1 \end{bmatrix}. \end{aligned} \tag{15}$$

For single frequency formulation, the tensor elements will be constant values. Thus, $\overline{\overline{M}}$ matrix consists of constant elements which have real and imaginary parts. For gyroelectric medium we have

$$\overline{\overline{M}} = \begin{bmatrix} \chi_{e1} & \chi_{e2} & & & & & \\ -\chi_{e2} & \chi_{e1} & & & & & \\ & & \chi_{e3} & & & & \\ & & & \chi_m & & & \\ & & & & \chi_m & & \\ & & & & & \chi_m & \\ & & & & & & \chi_m \end{bmatrix} \tag{16}$$

where χ_m is the magnetic susceptibility value. The matrix elements, which are not shown, have a value of zero. For gyromagnetic case the matrix $\overline{\overline{M}}$ has the form

$$\overline{\overline{M}} = \begin{bmatrix} \chi_e & & & & & & \\ & \chi_e & & & & & \\ & & \chi_e & & & & \\ & & & \chi_{m1} & \chi_{m2} & & \\ & & & -\chi_{m2} & \chi_{m1} & & \\ & & & & & \chi_{m3} & \end{bmatrix} \tag{17}$$

where χ_e is the electric susceptibility value. χ_m and χ_e are assumed to be real quantities.

In the field update equation

$$2\overline{F}^{e}_{scat} = 4\overline{F}_{scat} + s\Delta t\, 2\overline{\overline{M}}\,\overline{F}_{scat} + s\Delta t\, 2\overline{\overline{M}}\,\overline{F}_{inc} \tag{18}$$

when we multiply the matrix elements with $s\Delta t$ term, we will have

$$\begin{aligned} s\Delta t\chi_{e1} &= s\Delta t\Re[\varepsilon_1] + js\Delta t\Im[\varepsilon_1] \\ &= s\Delta t\Re[\varepsilon_1] - \omega\Delta t\Im[\varepsilon_1], \end{aligned} \tag{19}$$

$$\begin{aligned} s\Delta t\chi_{m1} &= s\Delta t\Re[\mu_1] + js\Delta t\Im[\mu_1] \\ &= s\Delta t\Re[\mu_1] - \omega\Delta t\Im[\mu_1], \end{aligned} \tag{20}$$

$$\begin{aligned} s\Delta t\chi_{e2} &= -s\Delta t\Im[\varepsilon_2] + js\Delta t\Re[\varepsilon_2] \\ &= -s\Delta t\Im[\varepsilon_2] - \omega\Delta t\Re[\varepsilon_2], \end{aligned} \tag{21}$$

$$\begin{aligned} s\Delta t\chi_{m2} &= -s\Delta t\Im[\mu_2] + js\Delta t\Re[\mu_2] \\ &= -s\Delta t\Im[\mu_2] - \omega\Delta t\Re[\mu_2], \end{aligned} \tag{22}$$

$$\begin{aligned} s\Delta t\chi_{e3} &= s\Delta t\Re[\varepsilon_3] + js\Delta t\Im[\varepsilon_3] \\ &= s\Delta t\Re[\varepsilon_3] - \omega\Delta t\Im[\varepsilon_3], \end{aligned} \tag{23}$$

$$\begin{aligned} s\Delta t\chi_{m3} &= s\Delta t\Re[\mu_3] + js\Delta t\Im[\mu_3] \\ &= s\Delta t\Re[\mu_3] - \omega\Delta t\Im[\mu_3] \end{aligned} \tag{24}$$

where $\Re[.]$ and $\Im[.]$ denote the real and imaginary parts of $[.]$, respectively. According to the derivations shown above, the term $s\Delta t2\overline{\overline{M}}$ can be decomposed into two parts as

$$s\Delta t2\overline{\overline{M}} = s\Delta t2\overline{\overline{X}}_1 + 2\overline{\overline{X}}_2 \tag{25}$$

where both $\overline{\overline{X}}_1$ and $\overline{\overline{X}}_2$ matrices have real valued elements and can be shown in explicit form for gyroelectric

medium as

$$\overline{\overline{X}}_1 = \begin{bmatrix} \Re[\varepsilon_1] & -\Im[\varepsilon_2] & & & & & \\ \Im[\varepsilon_2] & \Re[\varepsilon_1] & & & & & \\ & & \Re[\varepsilon_3] & & & & \\ & & & \chi_m & & & \\ & & & & \chi_m & & \\ & & & & & \chi_m & \end{bmatrix}$$

$$\overline{\overline{X}}_2 = -\omega\Delta t \begin{bmatrix} \Im[\varepsilon_1] & \Re[\varepsilon_2] & & & & & \\ -\Re[\varepsilon_2] & \Im[\varepsilon_1] & & & & & \\ & & \Im[\varepsilon_3] & & & & \\ & & & 0 & & & \\ & & & & 0 & & \\ & & & & & 0 & \end{bmatrix} \tag{26}$$

and for gyromagnetic medium as

$$\overline{\overline{X}}_1 = \begin{bmatrix} \chi_e & & & & & & \\ & \chi_e & & & & & \\ & & \chi_e & & & & \\ & & & \Re[\mu_1] & -\Im[\mu_2] & & \\ & & & \Im[\mu_2] & \Re[\mu_1] & & \\ & & & & & \Re[\mu_1] & \end{bmatrix}$$

$$\overline{\overline{X}}_2 = -\omega\Delta t \begin{bmatrix} 0 & & & & & & \\ & 0 & & & & & \\ & & 0 & & & & \\ & & & \Im[\mu_1] & \Re[\mu_2] & & \\ & & & -\Re[\mu_2] & \Im[\mu_1] & & \\ & & & & & \Im[\mu_1] & \end{bmatrix}. \tag{27}$$

Then (18) will become

$$\begin{aligned} 2\overline{F}^e_{scat} &= 4\overline{F}_{scat} + s\Delta t 2\overline{\overline{X}}_1\,\overline{F}_{scat} + 2\overline{\overline{X}}_2\overline{F}_{scat} \\ &\quad + s\Delta t 2\overline{\overline{X}}_1\,\overline{F}_{inc} + 2\overline{\overline{X}}_2\overline{F}_{inc} \end{aligned} \tag{28}$$

Then we apply the bilinear Z transform to (28) by changing

$$s\Delta t \to 2\frac{1-z^{-1}}{1+z^{-1}} \tag{29}$$

which yields to

$$\begin{aligned} 2\overline{F}^e_{scat} &= 4\overline{F}_{scat} + 4\tfrac{1-z^{-1}}{1+z^{-1}}\overline{\overline{X}}_1\,\overline{F}_{scat} + 2\overline{\overline{X}}_2\overline{F}_{scat} \\ &\quad + 4\tfrac{1-z^{-1}}{1+z^{-1}}\overline{\overline{X}}_1\,\overline{F}_{inc} + 2\overline{\overline{X}}_2\overline{F}_{inc}. \end{aligned} \tag{30}$$

After doing some algebra, (30) can be put in the following form.

$$\begin{aligned} (4\overline{\overline{I}} + 4\overline{\overline{X}}_1 + 2\overline{\overline{X}}_2)\overline{F}_{scat} &= 2\overline{F}^e_{scat} + z^{-1}\overline{S} \\ &\quad + (-4\overline{\overline{X}}_1 - 2\overline{\overline{X}}_2)\overline{F}_{inc} \end{aligned} \tag{31}$$

where

$$\begin{aligned} \overline{S} &= 2\overline{F}^e_{scat} + \left(4\overline{\overline{X}}_1 - 2\overline{\overline{X}}_2\right)\overline{F}_{inc} \\ &\quad + \left(-4\overline{\overline{I}} + 4\overline{\overline{X}}_1 - 2\overline{\overline{X}}_2\right)\overline{F}_{scat} \end{aligned} \tag{32}$$

$z^{-1}\overline{S}$ in Z domain corresponds to the previous time step information of $\overline{S}$ in time domain

$$\overline{S}(z) \to \overline{S}[n]\,,\; z^{-1}\overline{S}(z) \to \overline{S}[n-1]. \tag{33}$$

Here n is the time index. Hence we can write $z^{-1}\overline{S}$ as

$$\begin{aligned} \overline{S}[n-1] &= 2\overline{F}^e_{scat}[n-1] \\ &\quad + \left(4\overline{\overline{X}}_1 - 2\overline{\overline{X}}_2\right)\overline{F}_{inc}[n-1] \\ &\quad + \left(-4\overline{\overline{I}} + 4\overline{\overline{X}}_1 - 2\overline{\overline{X}}_2\right)\overline{F}_{scat}[n-1]. \end{aligned} \tag{34}$$

The scattered field update will be computed using

$$\overline{F}_{scat} = \overline{\overline{T}}\left(2\overline{F}^e_{scat} + (-4\overline{\overline{X}}_1 - 2\overline{\overline{X}}_2)\overline{F}_{inc} + z^{-1}\overline{S}\right) \tag{35}$$

where

$$\overline{\overline{T}} = \left(4\overline{\overline{I}} + 4\overline{\overline{X}}_1 + 2\overline{\overline{X}}_2\right)^{-1}. \tag{36}$$

In time domain

$$\begin{aligned} \overline{F}_{scat}[n] &= \overline{\overline{T}}\left(2\overline{F}^e_{scat}[n]\right) \\ &\quad + \overline{\overline{T}}\left((-4\overline{\overline{X}}_1 - 2\overline{\overline{X}}_2)\overline{F}_{inc}[n]\right) \\ &\quad + \overline{\overline{T}}\,\overline{S}[n-1]. \end{aligned} \tag{37}$$

In our computations, the region outside the scatterer is chosen to be free space, with $\overline{\overline{X}}_1 = 0$ and $\overline{\overline{X}}_2 = 0$. In the free space region, the incident field terms of (34) and (37) will drop (since $\overline{\overline{X}}_1 = 0$ and $\overline{\overline{X}}_2 = 0$) and only the scattered field terms will remain. This does not mean that the incident field is absent in the region. In our algorithm we only update the scattering fields in the free space region.

IV. Radar Cross Sections of Gyrotropic Spheres, Cubes and Cylinders

In this section, we will exhibit some of our TLM simulation results, where we modeled three dimensional homogeneous gyrotropic objects as our scatterers. For all our simulations, we imposed a TEM plane wave, whose electric field is polarized in x direction, as our incident field as shown in Fig. 1 for sphere. The scatterers are placed at the center of the computational space coinciding with the origin of the coordinate system. The radii of the spheres are denoted by a.

In our simulations we used a sinusoidal wave as the incident wave propagating in z direction, which has electric field component in x direction. The $\overline{F}_{inc}$ vector has the form of

$$\overline{F}_{inc} = \begin{bmatrix} V_{inc} \\ 0 \\ 0 \\ 0 \\ i_{inc} \\ 0 \end{bmatrix} \tag{38}$$

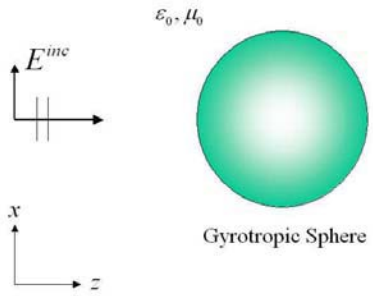

Fig. 1. Incidence of a plane wave to a gyrotropic sphere in free space.

where

$$V_{inc} = i_{inc} = -\Delta l \sin(2\pi f(n\Delta t - \frac{1}{c} z\Delta l)) \qquad (39)$$

n is the time step index and z is the z coordinate index of the cell. We have $-\Delta l$ in the front, since these quantities are normalized fields. V_{inc} in (38) denotes the E field in x direction, while i_{inc} represents the H field in y direction.

The results of bistatic RCS (radar cross section) calculations of gyrotropic spheres obtained by Geng et al. [1,2] and Zhu et al. [3], were reproduced using the TLM algorithm discussed before. Zhu et al. used the Method of Moments (MoM) speeded up with the Conjugate-Gradient Fast Fourier Transform (CG-FFT) approach. In [1] and [2], Geng et al. derived the scattering fields of eigenfunction representation in spectral domain, using the expansion of plane wave factors with the spherical vector wave function in isotropic media, and the Fourier Transformation. Since the results of the previous studies are for the total RCS (summation of co-polarization scattering and cross-polarization scattering) on E plane (the plane which is parallel to E^{inc}) and on H plane, which is perpendicular to the E plane, here we calculate the RCS of the same type in order to compare with the previous results.

First, we will examine a gyroelectric sphere, where the electrical dimension is chosen as $k_0 a = 0.5$ (k_0 is the free space wavenumber). Discretized space step Δl is set to be $a/20$ in our simulation. The time step Δt is equal to $\Delta l/2c$ for 3D TLM simulations, where c is the speed of light in free space, because the transmission lines connecting the nodes have an inductance per unit length of $\mu_0/2$ and a capacitance per unit length of $\varepsilon_0/2$. Thus, the velocity of propagation inside the transmission lines is $2c$. The relative permittivity tensor elements are assumed to be $\varepsilon_1 = 5$, $\varepsilon_2 = 1$, $\varepsilon_3 = 7$. On the other hand, the relative permeability of the sphere is assumed to be 1. Our simulation results are compared with those of Geng et al. in Fig. 2. The E plane is the xz plane, while the H plane is the yz plane. The results agree well with each other.

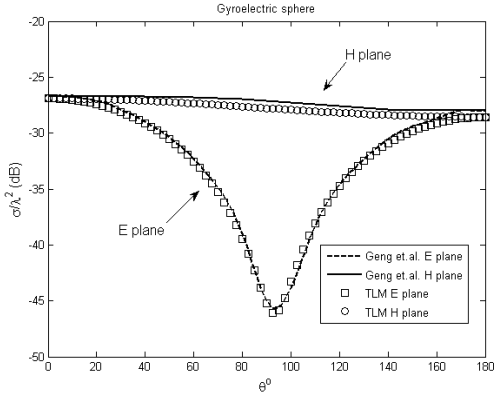

Fig. 2. Radar cross sections versus scattering angle θ. The results of TLM algorithm are shown along with the results of Geng et al. [1]. $k_0 a = 0.5$, $\varepsilon_1 = 5$, $\varepsilon_2 = 1$, $\varepsilon_3 = 7$ ($\Delta l = a/20$)

Another gyroelectric sphere with $k_0 a = \pi$ is considered. The relative permeability value is chosen to be 1, while the relative permittivity tensor elements are $\varepsilon_1 = 5.3495$, $\varepsilon_2 = -2$, $\varepsilon_3 = 7$. This example is also taken from the paper of Geng et al. [1]. The simulation was run with $\Delta l = \lambda/50$ (λ is free space wavelength). The agreement between the RCS results, which are plotted in Fig. 3, is reasonably good.

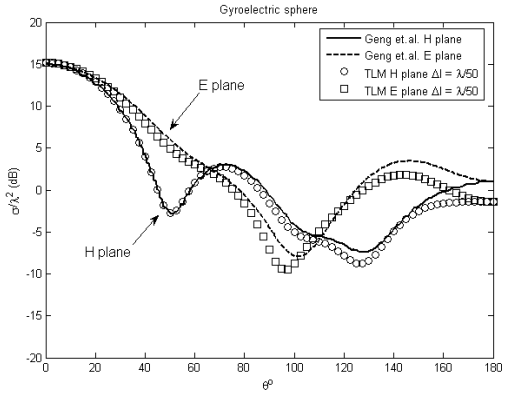

Fig. 3. Radar cross sections versus scattering angle θ. The results of TLM algorithm are shown along with the results of Geng et al. [1]. $k_0 a = \pi$, $\varepsilon_1 = 5.3495$, $\varepsilon_2 = -2$, $\varepsilon_3 = 7$ ($\Delta l = \lambda/50$)

Our next simulation case is a gyromagnetic sphere, where $k_0 a = 0.2\pi$. The discretized space step Δl is chosen to be $a/20$, and $\Delta t = \Delta l/2c$. The relative

permeability tensor elements are $\mu_1 = 5$, $\mu_2 = -1$, and $\mu_3 = 7$. Although, $\mu_3 = 7$ does not represent the ferrite material, we chose it to compare with the results of Geng et al.[2]. We assumed the relative permittivity of the sphere as 1. Fig. 4 shows the comparison of our simulation results with those of Geng et al.[2].

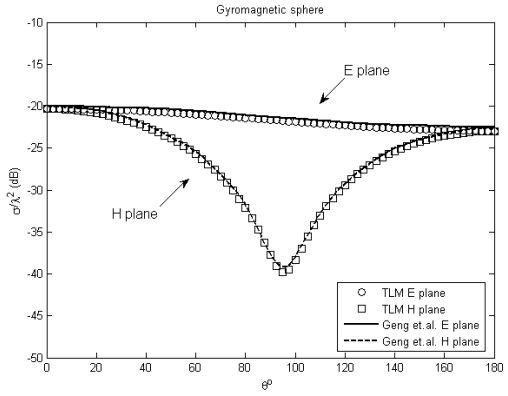

Fig. 4. Radar cross sections versus scattering angle θ. The results of TLM algorithm are shown along with the results of Geng et al. [2]. $k_0a = 0.2\pi$, $\mu_1 = 5$, $\mu_2 = -1$, $\mu_3 = 7$

As another simulation example, we modeled a gyromagnetic sphere with $k_0a = 2$, whose RCS was computed by Zhu et al. previously [3]. Similar to our previous sphere examples, we assumed a relative permittivity of 1. The relative permeability tensor elements are $\mu_1 = 1$, $\mu_2 = -1$ and $\mu_3 = 1$. $\Delta l = a/20$ and $\Delta t = \Delta l/2c$. Our RCS results agree well with the results obtained by Zhu et al. as shown in Fig. 5.

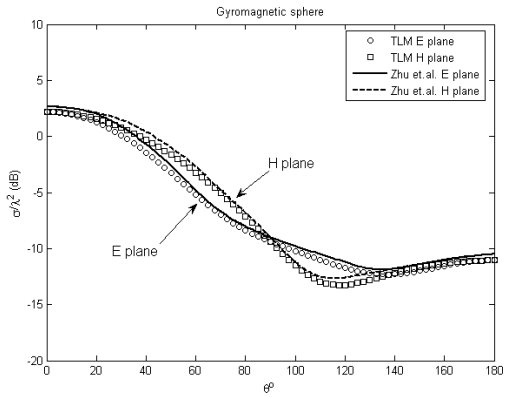

Fig. 5. Radar cross sections versus scattering angle θ. The results of TLM algorithm are shown along with the results of Zhu et al. [3]. $k_0a = 2$, $\mu_1 = 1$, $\mu_2 = -1$, $\mu_3 = 1$

It has been shown that our bistatic RCS results for gyrotropic spheres modeled using TLM algorithm agree well with the analytic bistatic RCS results of Geng et al. and MoM CG-FFT results of Zhu et al. As an advantage, our method is capable of simulating arbitrarily shaped, inhomogeneous objects. The radiation problems are also easy to implement with our technique.

Next, we will demonstrate the simulation of a gyroelectric cube. The incident field is x polarized plane wave traveling in z direction as shown in Fig. 6. In our computations the center of the cube coincides with the origin of the coordinate system. The length d of one side of the cube, is set to be 1.2λ, where λ is the wave length of the incident field.

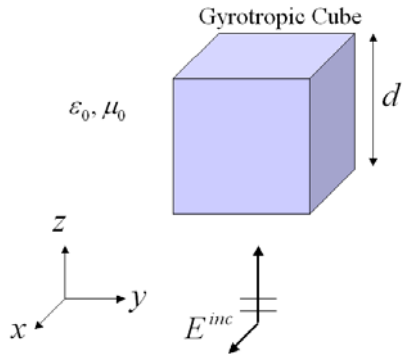

Fig. 6. Incidence of a plane wave on a gyrotropic cube in free space.

In our simulation $\Delta l = \lambda/30$ and $\Delta t = \Delta l/2c$. The permeability of the gyroelectric material is 1, while the permittivity tensor values are $\varepsilon_1 = 1$, $\varepsilon_2 = 1$ and $\varepsilon_3 = 1$. The bistatic RCS of the cube is given in Fig. 7.

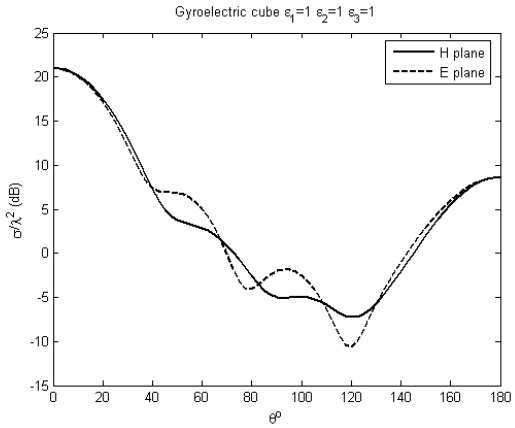

Fig. 7. Bistatic radar cross sections of the gyroelectric cube versus scattering angle θ. $d = 1.2\lambda$, $\varepsilon_1 = 1$, $\varepsilon_2 = 1$, and $\varepsilon_3 = 1$.

Keeping the dimensions of the cube as same as

gyroelectric case, we modeled a gyromagnetic cube, with a relative permittivity of 1. The relative permeability tensor elements are assumed as $\mu_1 = 1$, $\mu_2 = 1$ and $\mu_3 = 1$. The discrete time-step and space-step values are kept the same as gyroelectric cube case. Fig. 8 exhibits the bistatic RCS results of out TLM simulation for this gyromagnetic cube.

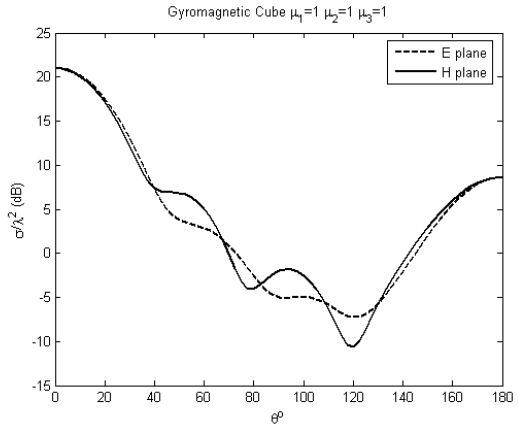

Fig. 8. Bistatic radar cross sections of the gyromagnetic cube versus scattering angle θ. $d = 1.2\lambda$, $\mu_1 = 1$, $\mu_2 = 1$, and $\mu_3 = 1$.

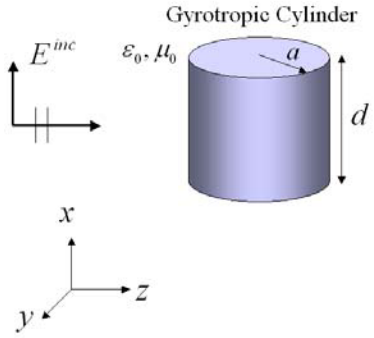

Fig. 9. Incidence of a plane wave on a gyrotropic finite cylinder in free space.

The finite circular cylinder is another special case in investigating the electromagnetic scattering of three dimensional gyrotropic objects. In our TLM simulations, we placed the gyrotropic cylinder as in Fig. 9, where the circular cross section is in y-z plane. An x polarized incident plane wave is traveling in z direction. The radius of the cylinder is denoted as a, while the height is represented by d.

We first modeled a gyroelectric cylinder, which has a height of $d = 1.2\lambda$ and a radius of $a = d/2$. We set $\Delta l = \lambda/30$ and $\Delta t = \Delta l/2c$. Our gyroelectric cylinder has a relative permeability of 1, while the relative permittivity tensor elements are $\varepsilon_1 = 1$, $\varepsilon_2 = 1$ and $\varepsilon_3 = 1$. The bistatic RCS of the cylinder is given in Fig. 10.

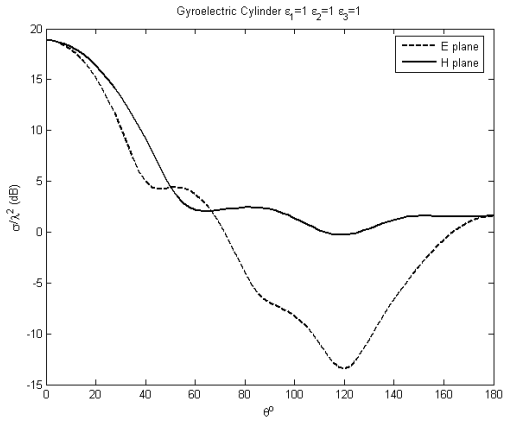

Fig. 10. Bistatic radar cross sections of the gyroelectric finite cylinder versus scattering angle θ. $d = 1.2\lambda$, $a = d/2$, $\varepsilon_1 = 1$, $\varepsilon_2 = 1$, and $\varepsilon_3 = 1$.

A gyromagnetic cylinder was simulated next, with the same discrete space-step and time-step as in gyroelectric cylinder case. The material has a relative permittivity value of 1. The relative permeability tensor elements are set as $\mu_1 = 1$, $\mu_2 = 1$ and $\mu_3 = 1$. The bistatic RCS of this cylinder is given in Fig. 11.

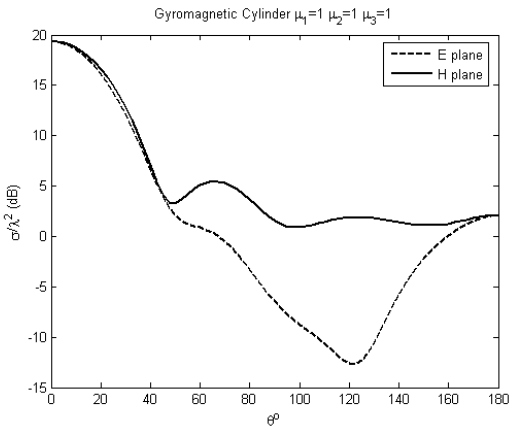

Fig. 11. Bistatic radar cross sections of the gyromagnetic finite cylinder versus scattering angle θ. $d = 1.2\lambda$, $a = d/2$, $\mu_1 = 1$, $\mu_2 = 1$, and $\mu_3 = 1$.

V. Conclusions

In this paper, the scattering field formulation of 3D TLM algorithm is derived starting from Paul's total field formulation TLM algorithm discussed in the [6]. Then

the gyrotropic material modeling for single frequency is explained. Moreover the near field to far field transformation with the notion of radar cross section is adapted to our TLM algorithm. The usage of this method is exhibited by modeling some gyrotropic spheres, cubes, and finite cylinders and computing the bistatic radar cross sections of these three dimensional scatterers. The TLM simulation results are validated by the results of the currently available methods used by Geng et al. [1,2] and Zhu et al. [3]. Using our method, it is easier to simulate arbitrarily shaped inhomogeneous gyrotropic objects.

ACKNOWLEDGMENTS

The authors wish to thank Dr. Atef Elsherbeni and Dr. Veysel Demir, for the valuable discussions on time domain electromagnetic computations.

REFERENCES

[1] Y. Geng, X. Wu, and L. W. Li, "Analysis of electromagnetic scattering by a plasma anisotropic sphere," *Radio Science*, vol. 38, no. 6, pp. 12/1–12/12, December 2003.

[2] Y. L. Geng and X. B. Wu, "A plane electromagnetic wave scattering by a ferrite sphere," *J. of Electromagn. Waves and Appl.*, vol. 18, no. 2, pp. 161–179, 2004.

[3] X. Q. Zhu, Y. L. Geng, and X. B. Wu, "Calculation of electromagnetic scattering from three-dimensional anisotropic objects (in Chinese)," *Chin. J. Radio Sci.*, vol. 17, pp. 209–215, 2002.

[4] K. S. Kunz and R. J. Luebbers, *The Finite Difference Time Domain Method for Electromagentics*. CRC Press, 1993.

[5] C. Christopoulos, *The Transmission Line Modelling Method TLM*. IEEE Press, 1995.

[6] J. Paul, "Modelling of general electromagnetic material properties in tlm," Ph.D. dissertation, University of Nottingham, 1998.

[7] J. Paul, C. Christopoulos, and D. W. P. Thomas, "Generalized Material Models in TLM – Part2: Materials with Anisotropic Properties," *IEEE Trans. on Antennas and Propagation*, vol. 47, no. 10, pp. 1535–1542, October 1999.

[8] V. Demir, "Electromagnetic scattering from three-dimensional chiral objects using the fdtd method," Ph.D. dissertation, Syracuse University, 2004.

[9] V. Demir, A. Z. Elsherbeni, D. Worasawate, and E. Arvas, "A graphical user interface (GUI) for plane wave scattering from a conducting, dielectric or a chiral sphere," *IEEE Antennas and Propagation Magazine*, vol. 46, no. 5, pp. 94–99, October 2004.

[10] H. C. Chen, *Theory of Electromagnetic Waves, Coordinate Free Approach*. McGraw Hill, 1983.

[11] V. L. Ginzburg, *The Propagation of Electromagnetic Waves in Plasmas*, 2^{nd} ed. Pergamon Press, 1970.

[12] A. Eroglu, "Electromagnetic wave propagation and radiation in a gyrotropic medium," Ph.D. dissertation, Syracuse University, 2004.

[13] A. F. Yagli, E. Arvas, and J. K. Lee, "Electromagnetic Scattering From Three-Dimensional Gyrotropic Objects at Single Frequency Using The TLM Method," *ACES Conference*, pp. 642–648, March 12–16 2006.

[14] H. H. Erkut, A. F. Yagli, and E. Arvas, "Electromagnetic scattering from a three-dimensional chiral body using the TLM method," *ACES Conference*, pp. 649–654, March 12–16 2006.

Ahmet Fazil Yagli was born in Kirikkale, Turkey, in 1979. He received the B.S. degree in Electrical and Electronics Engineering from Middle East Technical University, Ankara, Turkey in 2001, and the M.S. and Ph.D. degrees in Electrical Engineering from Syracuse University, Syracuse, NY in 2005 and 2006, respectively.

He served as a teaching assistant from August 2001 to May 2002, and as a research assistant from May 2002 to May 2006 in the Electrical Engineering and Computer Science Department of Syracuse University, Syracuse, NY. He is currently working for Turksat AS, Turkish Satellite Operator, in Ankara, Turkey. His research interests are in areas of computational methods for electromagnetics, radar cross section computation, and design and implementation of microwave devices.

Dr. Yagli is a member of ACES.

Jay Kyoon Lee was born in Sam-Chuk, Korea. He received the B.S. degree in Electronics Engineering from the Seoul National University, Seoul, Korea in 1976 and the S.M. and Ph.D. degrees in Electrical Engineering from the Massachusetts Institute of Technology (MIT), Cambridge, Massachusetts, in 1981 and 1985, respectively.

From 1976 to 1978, he served as an Operation Officer in the Air Defense Artillery Battalion of the Korean Army. He was employed by the Nam and Nam World Patent Office in Seoul, Korea in 1978-79. He was a Postdoctoral Research Associate at Research Laboratory of Electronics at MIT in 1985 and then joined the faculty of the Department of Electrical and Computer Engineering at Syracuse University in Syracuse, New York, where he is now Program Director of Electrical Engineering. He worked on the SAR imaging problem at Naval Air Development Center in Warminster, PA during summers of 1987 and 1988 and was a Visiting Professor at Rome Air Development Center in Rome, NY in 1990. He also worked at Naval Research Laboratory, Washington, DC during summer of 1993 and was an Invited Visiting Professor at Seoul National University in Seoul, Korea in 2000. His teaching and research interests include electromagnetic fields and waves, microwave remote sensing, waves in anisotropic

and gyrotropic media, antennas and propagation, microwave engineering, and radar clutter modeling. He has published numerous journal articles, book chapters and conference papers.

Dr. Lee is a Senior Member of the IEEE and a member of the American Geophysical Union, the Electromagnetics Academy and the Korean-American Scientists and Engineers Association (KSEA) in America. He has been on the International Editorial Board of Journal of Electromagnetic Waves and Applications since 1993. He has received the Eta Kappa Nu Outstanding Undergraduate Teacher Award from Syracuse University in 1999, the IEEE Third Millennium Medal in 2000, the College Educator of the Year Award from the Technology Alliance of Central New York in 2002 and the IEEE Region 1 Award in 2003. He has served as President of the Upstate New York Chapter of the KSEA in 1990-91, as Faculty Advisor of Korean Student Association at Syracuse University since 1993, as Chair of IEEE Syracuse Section in 1995-96, as Student Activities Committee Chair of IEEE Region 1 in 1996-2000, and as Faculty Advisor of IEEE Student Branch of Syracuse University since 1996.

Ercument Arvas received the B.S. and M.S. degrees from the Middle East Technical University, Ankara, Turkey, in 1976 and 1979 respectively, and PhD degree from Syracuse University, Syracuse, NY, in 1983, all in electrical engineering.

From 1984 to 1987, he was with the EE Department of Rochester Institute of Technology, Rochester, NY. In 1987, he joined the Electrical Engineering and Computer Science Department of Syracuse University, where he is currently a Professor. His research and teaching interests are in electromagnetic scattering and microwave devices.

He is a member of ACES and a Fellow of IEEE.